

# Experimental Study of Cavitation Characteristics of Axisymmetric Grooves(軸対称 戸溝のキャビテーション特性に関する実験的研究)

|     |   |
|-----|---|
| 著者  | TRUONG Anh Viet   |
| 号   | 3107  |
| 発行年 | 2003  |
| URL | <a href="http://hdl.handle.net/10097/8379">http://hdl.handle.net/10097/8379</a> |

氏名 チュン アン ビエット  
 授与学位 TRUONG Anh Viet 博士(工学)  
 学位授与年月日 平成16年3月25日  
 学位授与の根拠法規 学位規則第4条第1項  
 研究科, 専攻の名称 東北大学大学院工学研究科(博士課程) 機械知能工学工学専攻  
 学位論文題目 Experimental Study of Cavitation Characteristics of Axisymmetric Grooves  
 (軸対称戸溝のキャビテーション特性に関する実験的研究)  
 指導教官 東北大学教授 井小萩 利明  
 論文審査委員 主査 東北大学教授 井小萩 利明 東北大学教授 太田 照和  
 東北大学教授 上條 謙二郎

## 論文内容要旨

### Chapter 1 Introduction

The axisymmetric groove carved in a circular pipe is as the most popular structure of gate valve in pipe systems. The occurrence of cavitation always causes a serious erosive damage in this structure that becomes very important problem in the safety of engineering systems, especially at downstream of high-head dam, in pipe system of nuclei power plant, etc. But up to now, the cavitation occurrence in this structure is still not researched yet. Therefore, this study will intend to clarify the cavitation characteristics systematically in the series of axisymmetric groove models. The total 10 models with the variety of dimension scale and several irregular structures have been experimented for considering the characteristics of cavitation. The outline of the study is shown in Fig.1. In constitution, the thesis concludes of 8 chapters. The Chapter 1 introduces the related backgrounds and problems of cavitation study. The main content of experimental study is shown from Chapter 2 to Chapter 7. Chapter 8 is the general conclusion of present study.

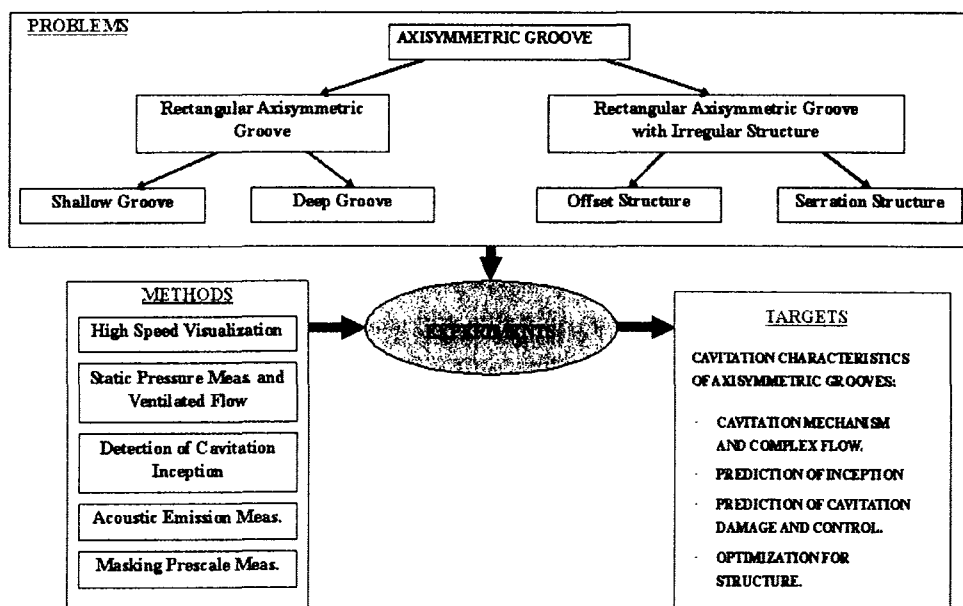


Fig.1 Outline of Present Study

## Chapter 2 Visualization of Cavitation in Axisymmetric Grooves

The occurrence of cavitation in axisymmetric rectangular groove is as the string of various types of cavitation phenomena in 2 zones, central area in groove space and groove downstream part. Depending on geometrical scale of groove, the cavitation process can be classified in 2 manners as followings:

(i) Cavitation process in the deep and square grooves;

*Incipient bubble cavitation* → *Cavitating vortex ring* + *Downstream traveling cavity* → *Groove supercavitating ring* + *Downstream sheet cavitation*

(ii) Cavitation process in the shallow grooves;

*Incipient bubble cavitation* → *Foggy cavity* → *Cloud cavity* + *Shear layer cavitation* + *Downstream sheet cavitation*.

The incipient cavitation is caused by the decreasing of local pressure at the core of vortices which driven by the shear layer flow separated from the upstream mouth of the groove.

In subcavitation state, the cavitating vortex ring (CVR) developed from initial bubble cavitation will appear at the central area of groove space when groove dimensional ratio  $D/B$  is in the range from 1 to 2. The shape of CVR is unaxisymmetric because of gravity force effect. The instability of vortex ring causes the shape of CVR having several waves. In shallow groove with dimensional ratio  $D/B < 1$ , CVR will does not appear, instead of that, the bubble cavitation is propagated in the form of foggy cavity. The traveling cavity is also appeared in the flow from groove cavitation zone to downstream.

In the most development of cavitation in ARG, the supercavitating vortex ring will occur to occupy entire groove space with a bulk of cloud cavity surrounding in the deep groove ( $D/B = 1 - 2$ ). Respectively, the cloud cavity and erosive shear layer vortex cavitation will occur at this stage of cavitation. Also in the developed cavitation stage, the high turbulent- and unstable- sheet cavity will be propagated in groove downstream from groove downstream edge. The cavity length much depends on the cavitation number  $\sigma$  in a power law. For the case of ARG with  $D/B = 1$ , the maximum cavity length  $L_{smax}$  can be predicted by the following formula:

$$L_{smax}/B = 3.71 \times (\Delta \sigma)^2$$

In scale effect, the cavity length is proportional with the depth  $D$  and reversed with the width  $B$  of groove.

## Chapter 3 Some Hydraulic Characteristics of Axisymmetric Grooves

The induced vortex flow pattern inside the groove much depends on groove dimensional ratio. In the  $D/B = 1$  groove, the flow pattern inside the groove is the vortex ring as a string of Rankine vortex. The structure of vortex flow is much affected by shear layer flow. The vortex-core velocity is direct proportional with friction velocity while the vortex circulation is a power function of shear flow Reynolds number  $R_{eB}$ .

In deep and shallow grooves, the vortex ring will be distorted in the type of 4- and 6-big-wave torus because the unstable of vortex core in vortex ring. The large shallow groove ( $D/B = 2$ ) can leads to the turbulent flow that makes the vortex ring very unstable and easy to be broken. On plane of circumference of distorted vortex ring in groove with  $D/B \neq 1$ , the vortex flow is in the type of several vortex pair which induced by wall jet flow as the result of impingement between shear layer flow and the downstream side wall of groove.

The generation of the vortex flow inside the groove causes a type of high fluctuation wall static pressure distribution along the wall of the groove. The stagnation zone is at the 4 corners of the groove. At downstream of the groove, the separation flow causes an inversed gradient pressure that leads the occurrence of sheet cavitation at this part.

## Chapter 4 Cavitation Inception in Axisymmetric Grooves

The incipient vortex cavitation caused by the low pressure at vortex core is much effected by gas content of water. While the incipient sheet cavitation is caused by separation flow at groove downstream edge. The law for the case of groove with geometric scale  $D/B = 1$  is predicted by the following formula:

$$\sigma_i = -C_{p \min} + \frac{k_g \alpha_1 \beta}{\frac{1}{2} \rho U_\infty^2}$$

Where, gas diffusion coefficient  $k_g = 0.85$  determined by the experiment in the air content of water  $\alpha/\alpha_s = 1.1$ .

The semi-empirical formula is also introduced for both type of cavitation inception as below:

(a) For incipient vortex cavitation of the cavitating vortex ring:

$$\sigma_{iv} = 3.036 \times 10^4 R_{eB}^{-1.38} + \frac{K \alpha \beta}{\frac{1}{2} \rho U_\infty^2}$$

here,  $K = 0.131(\log R_{eB})^2 - 0.412 \log R_{eB} + 0.586$

(b) For incipient sheet cavitation at the back groove edge:

$$\sigma_{is} = 70.6 R_e^{-0.47} + \frac{K_s \alpha \beta}{\frac{1}{2} \rho U_\infty^2}$$

Here,  $K_s = 0.017(\log Re)^2$ .

In the change of groove dimensional ratio in the range of  $D/B = 0.5$  to 2, the incipient vortex cavitation performance is not changed significantly, but the sheet cavitation inception is much effected by dimension scale. The scaling law has been made for prediction of this inception as following:

$$\sigma_{is} = \left(\frac{B}{D}\right)^{0.38} \left(\frac{B}{R}\right)^{0.29} F(R_e)$$

with  $F(Re)$  is a power function of Reynolds number that may depend on the effect of water temperature. At temperature around  $T = 21^\circ\text{C}$ , the law can be written as in the formula:

$$\sigma_{is} = 9.16 \times 10^6 \left(\frac{B}{D}\right)^{0.38} \left(\frac{B}{R}\right)^{0.29} R_e^{-1.22}$$

The effect of temperature is predicted that the inception cavitation number will increase in the high temperature.

## Chapter 5 Acoustic Emission of Cavitation in Axisymmetric Grooves

The acoustic emission (AE) signal can be used as the effective tool for indirect detection and control of cavitation. The range of AE frequency of cavitating flow in ARG is from 4 to 20 kHz. The typical spectra is a 2 main peak curve with the sagging point around 7 kHz for the sensor position located at the top groove and 8.6 kHz for 2 sensors at near groove up- and downstream.

In tendency, the relationship between impulsive pressure and cavitation number  $\sigma$  is alike power function in the same trend of AE RMS measurement that confirms the possibility of AE detection in cavitation damage. Only the high amplitude AE signal may relate to erosion intensity of cavitating flow.

## Chapter 6 Erosion Damage of Cavitation in Axisymmetric Grooves

The concentrated collapse area of cavitation on wall surface in axisymmetric grooves is concluded 3 main parts, such as, (i) Downstream side wall of groove; (ii) Groove bed and (iii) Groove downstream.

The impulsive collapse area (i) on the downstream side wall of groove is much related to the strength of shear layer vortex cavitation. The decreasing of groove width can reduce and omit the appearance of this impact area in both aspects of pressure intensity and geometric scale. The relationship between the width  $W$  of impact area and Reynolds number  $R_e$  is linear in the detectable range of  $R_e = 4 \times 10^5$  to  $10^6$  and  $W$  is also in linear proportion with the relative groove width  $B/R$ . The highest erosion damage is at the widest shallow groove S3 ( $D/B=0.5$ ), and this damage seem to be disappeared in the deep groove D2 ( $D/B=2$ ).

The concentrated impact area (ii) on groove bed is intermittent in 3 main types, such as, (1) single line; (2) double line and (3) "V" shape. The distance between impulsive lines depends on the Reynolds number that the number of impulsive lines is increasing when  $R_e$  is increasing. This number  $N$  is expected to relate with the waves induced by the vortex ring flow in the effects of groove wall, especially the impingement of shear layer flow on the downstream side wall of groove.

## Chapter 7 Cavitation Characteristics in Axisymmetric Groove with Some Irregularities of Structure

The irregular structure can make some remarkable changes in the intensity of cavitation as well as the cavitation phenomenon.

In groove with upstream offset structure, the break-off of CVR may eliminate erosion damage on groove at high Reynolds number but the formation of cavitating jet with the super-sheet cavitation can cause severe erosion in groove far downstream.

The conical downstream structure shows a good cavitation performance, at least is the best structure in 4 detected grooves. By this structure, sheet cavitation is eliminated. The impulsive pressure intensity on groove wall and downstream part is lowest in 4 models.

The vortex flow pattern in grooves with upstream off-set and conical downstream pipe is similar to the case of groove  $D/B = 1$ , that is the string of Rankine vortex, but these structure cause a higher vortex intensity. The cavitation inception in these 2 case is also experienced in good agreement by the same law of gas diffusion coefficient  $k_g$  by 0.85.

In serration models, the upstream serrated edge does not make significant change in performance of cavitation. But the downstream serrated edge makes a significant change the type of attached cavitation at groove downstream with the appearance of streak cavitation. The attached cavity is generated from the hollow-angle edge of serration and fluctuating at downstream. The interaction of streak cavities causes a high erosive pressure concentration along downstream surface.

## Chapter 8 General Conclusion

The carried out characteristics of cavitation of these cases upgrades the knowledge in the mechanism of cavitating flow as well as cavitation control and for optimization in design of axisymmetric groove structure, especially in gate vane. The axisymmetric deep groove with the downstream conical structure is considered as the best solution for avoiding cavitation damage.

# 論文審査結果の要旨

ダム等の水理施設における配管系には、大流量調節のために大型の仕切弁やゲート弁等が設置されている。通常、弁全閉時には弁体が管路の周囲に設けられた戸溝に密閉され水流を完全に遮断する構造になっているが、弁全開時にこの戸溝のまわりにキャビテーションが発生し、しばしばキャビテーション壊食の危険性にさらされる。一度キャビテーションにより戸溝が破損すると地下施設のためその補修あるいは取替えには多大な費用を要する。このため、戸溝まわりキャビテーションの挙動を明らかにし、その健全性の向上を図ることは極めて重要である。本論文は水平直円管に設けた各種形状の軸対称戸溝まわりに発生するキャビテーション特性を実験的に究明し、健全性向上のための方策を検討した結果をまとめたもので全編8章よりなる。

第1章は序論である。

第2章では、戸溝の幅 $B$ と深さ $D$ を変化させた短形断面の各種モデルに発生するキャビテーションの様相を瞬間写真やレーザーライトシートを用いた高速ビデオにより観察し、戸溝内での初生キャビテーションと発達した渦輪キャビテーションの非定常挙動、下流側の戸溝外縁から発生するシートキャビティなどの3次元キャビテーション流れ構造を明らかにしている。特に、 $B/D < 1$ の深い戸溝では渦輪キャビテーションが発達するが、 $B/D > 1$ の浅い戸溝では明瞭な渦輪が消失するなど、戸溝形状による発達形態の相違を見出している。

第3章では、非キャビテーション状態において戸溝外縁直前から注入した微小空気泡の流跡線を高速ビデオで追跡し、戸溝内の渦輪構造を明らかにしている。すなわち、渦輪の周方向にはいくつかの渦対からなるらせん構造が見てとれ、渦輪が明瞭な $B/D=1$ の場合の渦輪断面内の渦循環分布はほぼランキン渦で近似できることを示している。

第4章では、戸溝内の渦輪キャビテーションと下流側の戸溝外縁からのシートキャビテーションの初生則を論じている。初生はそれぞれ最低圧力とヘンリー則に基づく溶存空気の拡散によって支配され、初生キャビテーション係数の半経験式を各種モデルの寸法効果も考慮して提示している。これは、戸溝のキャビテーションに対する健全性を評価する一つの指標として有用な成果である。

第5章ではアクリル製戸溝流路の外壁に設置したAEセンサを用いて、各種モデルにおけるAE信号を解析し、種々のAE特性をキャビテーション係数 $\sigma$ に対して明らかにしている。 $\sigma < 1$ の範囲で、AE強度が指数的に増大し、壊食の危険性が生ずることを特定している。

第6章では、防水型感圧紙を用いて、戸溝内壁面および戸溝下流の管路内壁面上の衝撃圧分布を測定している。その結果、上流側の戸溝外縁からのはく離せん断流が衝突する下流側の戸溝側面、戸溝底面および下流側の戸溝外縁から発生するシートキャビティの崩壊が起こる管路内壁面上の3ヶ所に顕著な衝撃圧分布が存在することを確認している。特に、戸溝底面の衝撃圧分布は、ほぼ等間隔の特異な縞模様を呈し、らせん構造を有する渦輪キャビテーションの収縮膨張に起因することを示唆している。これらは、戸溝の壊食軽減策を見出す上で重要な知見である。

第7章では、上流側の戸溝外縁にセレーションと突起を、下流側の戸溝外縁にセレーションと円錐状の面取りをそれぞれ施した4種のモデルを用いて、上記の各章と同様にキャビテーション特性を考察している。その結果、原型の短形断面の戸溝に比し、下流側の戸溝外縁に面取りを施すことにより、第6章で確認された3ヶ所の衝撃圧がいずれも最も軽減されることを見出している。これは、実用上有用な知見である。

第8章は結論である。

以上要するに本論文は短形断面の軸対称戸溝まわりに発生するキャビテーション特性を解明するとともに、壊食の軽減に好適な戸溝形状を提示したもので機械工学および流体工学の発展に寄与するところ少なくない。よって、本論文は博士(工学)の学位論文として合格と認める。